Proceedings of HTFED2004
2004 ASME Heat Transfer/Fluids Engineering Summer Conference
Charlotte, North Carolina, USA July 11-15, 2004

HT-FED2004-56745

ANALYTICAL MODELS FOR SYSTEMATIC ERRORS OF DIFFERENTIAL SCANNING CALORIMETRY INSTRUMENTS

Adrian S. Sabau and Wallace D. Porter
Oak Ridge National Laboratory; Oak Ridge, TN 37831-6083, USA

ABSTRACT

Differential Scanning Calorimetry (DSC) measurements are routinely used to determine enthalpies of phase change, phase transition temperatures, glass transition temperatures, and heat capacities. In order to obtain data on the amount of phases during phase change, time-temperature lags, which are inherent to the measurement process, must be estimated through a computational analysis. An analytical model is proposed for the systematic error of the instrument. Numerical simulation results are compared against experimental data obtained at different heating and cooling rates.

"Keywords: Heat Flux Differential Scanning Calorimeter, temperature lag, analytical model".

INTRODUCTION

The temperature lags are inherent to the DSC measurement systems since (a) temperatures are recorded from thermocouples that are placed away from the sample and reference materials (Figure 1), and (b) there is a non-homogeneous temperature distribution within the DSC instrument. By performing a computational analysis of the measurement process, the temperature lags can be estimated and their effect can be taken into account in determining the thermophysical properties.

Gray (1968) proposed one of the first models to describe the heat flow in DTA cells that has been adopted for the study of DSC instruments.

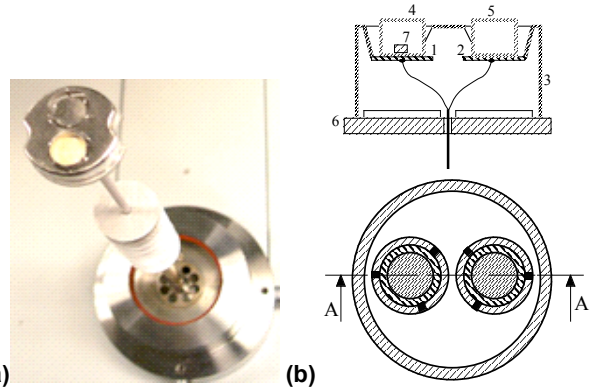

Figure 1. Sensing system for typical heat flux type DSC system used for high-temperature applications: (a) picture and (b) schematic.

Dong and Hunt (2001) developed an analytical model for the DSC heat flux instrument by considering that the instrument can be represented by a certain number of regions of uniform temperatures. However, their model includes some heat transfer features that do not exist in the instrument, such as conduction paths between the sample plates and furnace. Kempen et al. (2003) modeled the Netzsch DSC 404C heat flux instrument using an oversimplified heat transfer model, e.g., only the plates and pans are considered in the model and a conduction path between the sample plates and furnace is considered.

The Netzsch DSC 404C heat flux instrument is considered in this study (Figure 1). Sabau et al. (2004) presented a system of nonlinear ordinary differential equations, which accounts for the conduction and radiation heat transfer within all the parts in the instrument. The results presented were in good agreement with experimental results for the reference plate temperature. However, the results for the difference between the sample plate temperature, *Ts*, and reference plate temperature, *Tr*, are not in agreement with experimental results. This poor agreement with experimental data for *Ts*-*Tr* showed that the time constants of the model cannot alone handle the systematic error in the instrument.

The effect of the systematic error, or instrument asymmetry, is evidenced as a nonzero variation of the *Ts*-*Tr* for baseline measurements, i.e. when either no pans or pans without samples were used. Experiments indicate that the instrument asymmetry is due to (a) the mass difference between the sample side and reference side and (b) different time constants for the thermocouple assemblies on the sample and reference sides. Numerical simulation results showed that the mass difference between the sample and reference containers accounts for a small part of the instrument asymmetry. Danley (2003) introduced a new DSC sensor design and a new method for reducing the baseline. Their method comprises two differential temperature measurements instead of one and an additional temperature measurement.

A close look at the sensing unit reveals other sources of intrinsic differences between the sample and reference side that can yield a signal difference between the two sides of the instrument. By changing the position of the sensing unit inside the furnace, the systematic error may decrease but it cannot be removed. On the other hand, certain nonuniform

temperature distribution of the furnace wall is expected as well as a non-homogeneous temperature distribution within the DSC instrument such that the sample and reference plates are not at the same temperature. These geometric effects cannot be considered through simple conduction and radiation mechanisms between instrument parts. In this paper, a model is presented for instrument asymmetry that was developed based on measurements conducted at different heating and cooling rates.

CONSTITUTIVE EQUATIONS FOR THE DSC INSTRUMENT

Temperatures are normalized with respect to the initial temperature, i.e., $y=T/T_o$. The most complex model, which includes all the heat transfer interactions between different components of the DSC sensing unit, is shown in Table I. The mathematical model is based on the assumption that each component is isothermal and that the heat transfer among components occurs by conduction and radiation. The thermal resistances in the system are represented by effective conduction time constants, τ_C, and radiation time constants, τ_R. An analysis of the model features was presented by Sabau et al. (2004) with the aim of formulating one of the simplest models that can qualitatively reproduce all the typical features of a DSC signal.

In Table I, c_k are specific heat terms defined as: $c_k = C_p^k(y_k)/C_p^k(1)$, $c_{f7} = \left(-L_7/T_0 + y_m\left(C_p^{7,L} - C_p^{7,S}\right)\right)/C_p^7(1)$, where L_7 is the latent heat of the sample material, $C_p^{7,L}$ is the specific heat of the liquid metal at the melting point, $C_p^{7,S}$ is the specific heat of the pure metal in the solid state at the melting point. For pure metal or eutectic alloys, the phase change occurs at a single temperature, T_m, and $y_m = T_m/T_0$. During the phase change, the sample temperature is considered constant while its solid fraction varies according to the energy balance within that time step. Since the controller thermocouple is located away from the furnace walls, a temperature lag between the controller temperature and furnace wall temperature was considered.

The set point temperature is defined as the temperature set by the operator and is usually a linear variation in time given by the constant heating or cooling rate, i.e., $y_P(t) = 1 + \sum_{n=1}^{N} \alpha_n (t - t_n) H(t - t_n)$, where H is the Heaviside function. $\alpha_n = R_n/T_0$ where R_n is the heating and/or cooling rate [C/s]. The disk, reference container and sample container are made of alumina while the other parts are made of a platinum alloy.

INITIAL CONDITIONS

In the results presented by all studies, there is no discussion on the initial conditions. In most of studies, such as those by Dong and Hunt (2001) and Boettinger and Kattner (2002), the numerical simulation results are presented for a certain temperature interval around the solidus and liquidus temperatures, without providing any information on the initial conditions.

If the simulations start at room temperature, the initial conditions are known and the model has to be accurate enough to deal with the inherent transient phenomena.

Table I. Analytical model of the DSC instrument.

$$\frac{dy_0}{dt} = \frac{y_P - y_0}{\tau_{CF}}$$

$$c_1 \frac{dy_1}{dt} = \frac{y_3 - y_1}{\tau_{C1}} + \frac{y_3^4 - y_1^4}{\tau_{R1}} + \frac{y_4 - y_1}{\tau_{C3}} + \frac{y_6^4 - y_1^4}{\tau_{R4}}$$

$$c_2 \frac{dy_2}{dt} = \frac{y_3 - y_2}{\tau_{C2}} + \frac{y_3^4 - y_2^4}{\tau_{R1}} f_1 + \frac{y_5 - y_2}{\tau_{C4}} + \frac{y_6^4 - y_2^4}{\tau_{R4}} f_1$$

$$c_3 \frac{dy_3}{dt} = \frac{y_1 - y_3}{\tau_{C1}} f_2 + \frac{y_2 - y_3}{\tau_{C2}} \frac{f_2}{f_1} + \frac{y_0^4 - y_3^4}{\tau_{R2}} + \frac{y_6^4 - y_3^4}{\tau_{R5}}$$

$$c_4 \frac{dy_4}{dt} = \frac{y_1 - y_4}{\tau_{C3}} f_3 + \frac{y_0^4 - y_4^4}{\tau_{R3}} + \frac{y_8 - y_4}{\tau_{C5}} f_{10} + \frac{y_5^4 - y_4^4}{\tau_{R8}}$$

$$c_5 \frac{dy_5}{dt} = \frac{y_2 - y_5}{\tau_{C4}} f_4 + \frac{y_0^4 - y_5^4}{\tau_{R3}} f_5 + \frac{y_7 - y_5}{\tau_{C6}} f_8 + \frac{y_4^4 - y_5^4}{\tau_{R8}} f_5$$

$$c_6 \frac{dy_6}{dt} = \frac{y_3^4 - y_6^4}{\tau_{R5}} f_6 + \frac{y_0^4 - y_6^4}{\tau_{R6}} f_7 + \frac{y_{sce} - y_6}{\tau_{C7}} + \frac{y_{sce}^4 - y_6^4}{\tau_{R7}}$$

$$c_7 \frac{dy_7}{dt} + c_{f7} \frac{df_{S7}}{dt} = \frac{y_5 - y_7}{\tau_{C6}} f_9,$$

$$c_8 \frac{dy_8}{dt} = \frac{y_4 - y_8}{\tau_{C5}} f_{11}$$

The components have the following mass: m_1=0.103, m_2=0.103, m_3=1.21, m_4=0.2481, m_5=0.2437, m_6=1.53 [g]. The mass factors in the analytical DSC model are given as:

$$f1 = m1/m2,\ f2 = m1/m3,\ f3 = \frac{m_1 C_p^1(1)}{m_4 C_p^4(1)},\ f4 = \frac{m_2 C_p^2(1)}{m_5 C_p^5(1)},\ f5 = m4/m5,$$

$$f6 = \frac{m_3 C_p^3(1)}{m_6 C_p^6(1)},\ f7 = 1,\ f8 = 1,\ f9 = \frac{m_5 C_p^5(1)}{m_7 C_p^7(1)},\ f10 = 1,\ f11 = \frac{m_4 C_p^4(1)}{m_8 C_p^8(1)}.$$

If the simulation starts at high temperature, say $T_{solidus}$-100°C, then the initial conditions for all components are not known and assumptions on their values must be made. The transition between heating and cooling regime is another transient regime that occurs inevitably. It is yet to be seen how well the models, which are based on isothermal body assumption, perform in these transient regimes since at least the furnace undergoes changes that makes its temperature highly non isothermal.

MODEL FOR SYSTEMATIC INSTRUMENT ERROR

The instrument asymmetry is dependent on temperature and temperature rate. Also, the variation of instrument asymmetry during changes in temperature rate show typical lags that can be described with time constant-like equations. Various formulations have been tried to consider the instrument asymmetry. The formulation presented by Osborne et al. (2004), does not take into account the temperature rate dependence. As the asymmetry is present for

runs when no containers are used, the asymmetry was then modeled as a source term to the sample plate equation. This source-term formulation failed to describe the heating rate dependence. In order to account for the asymmetry, the following model is proposed for the temperature difference between the sample side and reference side, *Ts-Tr*:

$$\begin{aligned} T_S - T_R &= T_2 - T_1 + \varepsilon_A \\ \frac{d\varepsilon_A}{dt} &= \frac{\varphi - \varepsilon_A}{\tau_A} \\ \varphi(y_0,\alpha) &= (y_0 - 1)(g_1\,\alpha - g_0) \end{aligned} \qquad (1)$$

where, ε_A is the asymmetry term. In order to account for the rate dependence, the evolution of the asymmetry term is described by a time constant-like equation. τ_A is a time constant whose values should be close to the furnace time constant, $\tau_{CF.}$ α is the heating rate while g_1 and g_0 are constant parameters. The following parameters were found to give one of the best agreement for *Ts-Tr*: τ_A=40s, g_0=0.0011, and g_1=2.22 [s].

NUMERICAL SIMULATION RESULTS

The computational results were compared against experimental data for baseline runs, i.e., empty containers, and sample runs using pure aluminum. The several cases considered are identified in Table II. The baseline cases and sample cases are labeled with letter *B* and *S*, respectively, followed by the case number. Based on experimental and computational results most critical model features were identified in order to reproduce all the typical features of a DSC signal. Initially, experiments were performed at heating rates of 20°C/min from room temperature until the set point reached a temperature of 1073K following by cooling with 20°C/min. For each case, the same model parameters were considered. The representative parameters for each case are shown in Table III. Sabau et al., (2004) showed that for this model there was a good fit for the reference temperature results. However, the results for the temperature difference, *Ts-Tr*, between the sample plate temperature and reference plate temperature, showed very poor agreement since the instrument asymmetry was not considered.

In this section, only results for the *Ts-Tr* will be presented. In Figure 2a, *Ts-Tr* is shown for the temperature range common to all cases considered. There is a very good agreement with experimental results for baseline runs. For sample runs, computational results show larger values at low temperatures. At higher temperatures, there is a good agreement with experimental results for baseline runs as well as for sample runs for all cases considered (Figure 2b, 3a, and 3b). However, the position of the peaks at cooling, which were due to phase change were observed at higher temperatures. These results provide an experimental validation of the proposed asymmetry formulation since the *Ts-Tr* data were reproduced during the transition to different heating rates and cooling rates.

The significance of our results can be explained by considering the data for the baseline run and sample run. We can note that since the asymmetry factor, ε_A, depends on the furnace temperature, it is the same for baseline run and sample run conducted with the same heating and cooling rates. Thus, based on the asymmetry equations, we can obtain that:

$$[T_S - T_R]_S - [T_S - T_R]_B = [T_2 - T_1]_S - [T_2 - T_1]_B. \qquad (2)$$

In standard DSC practice, this subtraction of the baseline results from the sample results, i.e., $[T_S - T_R]_S - [T_S - T_R]_B$, is performed to determine the specific heat. The same subtraction is also used in all the numerical simulation studies in order to eliminate the asymmetry effects, where it is assumed that the calculated temperature difference, $[T_2 - T_1]_S$, is exactly $[T_S - T_R]_S - [T_S - T_R]_B$. However, as it can be seen from the equation 2, this assumption may not be true.

Table II. Cases considered for numerical simulations.

Case id	Heating rate [°C/min]	Temperature [°C] /Time [s] when heating rate changes	Heating rate [°C/min]	Temperature [°C] /Time [s] at heating-cooling transition	Cooling rate [°C/min]	Case type
B1	20	-	20	800/2324.7	20	baseline run
S1	20	-	20	800/2324.7	20	sample run
B2	20	600/1724.7	10	800/2924.7	10	baseline run
S2	20	600/1724.7	10	800/4124.7	10	sample run
B3	20	600/1724.7	5	800/4124.7	5	baseline run
S3	20	600/1724.7	5	800/4124.7	5	sample run

Table III. Time constants [s] for cases considered for numerical simulations.

Radiation parameters							Furnace	Stem parameters	
τ_{R1}	τ_{R2}	τ_{R3}	τ_{R4}	τ_{R5}	τ_{R6}	τ_{R8}	τ_{CF}	τ_{C7}	τ_{R7}
650	1000	680	220	200	6300	4000	30	2500	30000

The following conduction parameters were considered $\tau_{C1}=\tau_{C2}=3.3$, $\tau_{C3}=\tau_{C4}=0.01$, $\tau_{C5}=1$, $\tau_{C6}=10$ *s*.

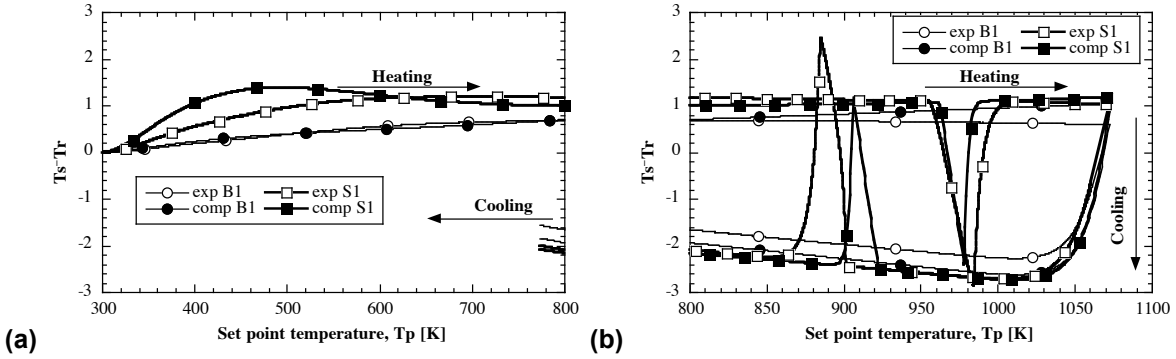

Figure 2. Temperature difference between the sample plate and reference plate for cases B1 and S1 for temperature domains of (a) [300:800] K and (b) [800:1100] K.

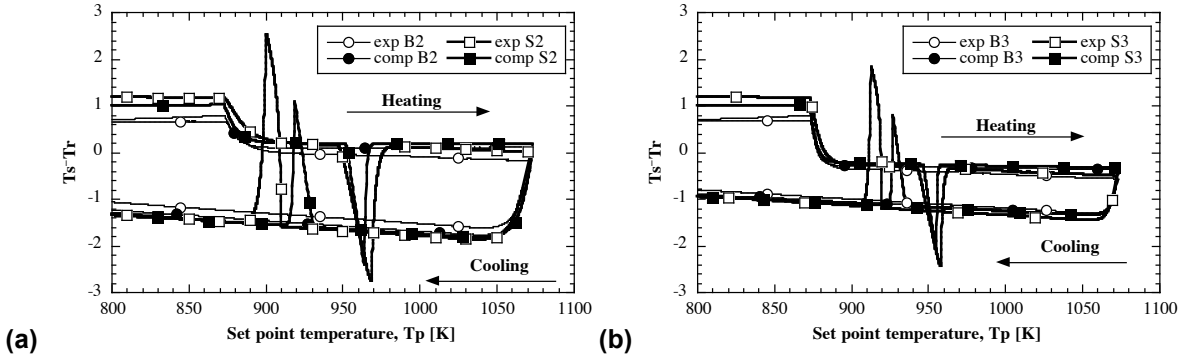

Figure 3. Temperature difference between the sample plate and reference plate for the high temperature domain [800:1100] K: (a) cases B2 and S2 and (b) cases B3 and S3.

SIMPLIFIED DSC MODELS

The model shown in Table 1 requires numerous parameters. Some of these physical parameters can be determined from experiments while others can be determined by performing an inverse analysis of parameter-estimation type. In order to describe the system with less number of components, an attempt is made to simplify the model by excluding the large container and alumina disk from the analysis (Table IV). In this case, we assume that the plates and containers exchange heat from a furnace medium of dimensionless temperature y_0. The heat losses through the stem are now dealt with as heat losses to the ambient. A new temperature is introduced, the controller temperature, y_C. In the experiments conducted, a thermocouple embedded in the furnace walls is used to control the instrument heaters such that its temperature follows the set point temperature. In Table IV it is assumed that the controller temperature lags that of the set point and that there are heat losses to the ambient temperature, y_a.

For the controller-furnace model shown in Table IV, the time-constant parameters that yield similar results to those in Figures 2 and 3 are: $\tau_{C1}=\tau_{C2}=3$, $\tau_{C3}=\tau_{C4}=2$, $\tau_{C5}=1$, $\tau_{C6}=10$ *s*, τ_{R1}=800, τ_{R3}=2000, τ_{R5}=200, τ_{R6}=6,300, τ_{R8}=4,000,

Table IV. Analytical model of the DSC instrument based on furnace and controller temperatures.

$$\frac{dy_c}{dt}=\frac{y_p-y_c}{\tau_{CF}}+\frac{y_p^4-y_c^4}{\tau_{RF}}+\frac{y_a-y_c}{\tau_{Ca}}+\frac{y_a^4-y_c^4}{\tau_{Ra}}$$

$$\frac{dy_0}{dt}=\frac{y_c-y_0}{\tau_{CF1}}+\frac{y_c^4-y_0^4}{\tau_{RF1}}$$

$$c_1\frac{dy_1}{dt}=\frac{y_0-y_1}{\tau_{C1}}+\frac{y_0^4-y_1^4}{\tau_{R1}}+\frac{y_4-y_1}{\tau_{C3}}$$

$$c_2\frac{dy_2}{dt}=\frac{y_0-y_2}{\tau_{C2}}+\frac{y_0^4-y_2^4}{\tau_{R1}}f_1+\frac{y_5-y_2}{\tau_{C4}}$$

$$c_4\frac{dy_4}{dt}=\frac{y_1-y_4}{\tau_{C3}}f_3+\frac{y_0^4-y_4^4}{\tau_{R3}}+\frac{y_8-y_4}{\tau_{C5}}f_{10}+\frac{y_5^4-y_4^4}{\tau_{R8}}$$

$$c_5 \frac{dy_5}{dt} = \frac{y_2 - y_5}{\tau_{C4}} f_4 + \frac{y_0^4 - y_5^4}{\tau_{R3}} f_5 + \frac{y_7 - y_5}{\tau_{C6}} f_8 + \frac{y_4^4 - y_5^4}{\tau_{R8}} f_5$$

$$c_7 \frac{dy_7}{dt} + c_{f7} \frac{df_{S7}}{dt} = \frac{y_5 - y_7}{\tau_{C6}} f_9,$$

$$c_8 \frac{dy_8}{dt} = \frac{y_4 - y_8}{\tau_{C5}} f_{11}$$

τ_{R1}=800, τ_{R3}=2000, τ_{R5}=200, τ_{R6}=6,300, τ_{R8}=4,000, τ_{Ca}=*N/A*, τ_{Ra}=80,000, τ_{CF}=*60*, τ_{RF}=7000, τ_{CF1}=*120*, τ_{RF1}=2,000, τ_A=40s, g_0=0.33, and g_1=79.3 [s].

Although the interactions between instrument components are minimized in the controller-furnace model, the deficiencies noted with the first model are not corrected. Numerical simulation results indicate that the furnace temperature plays an important role in the model. However, there is no simple approach to account for furnace temperature variation. The furnace temperature should be described by using more time constants than the two models considered, which will increase the complexity of the model.

INSTRUMENT UNCERTAINTIES

In order to document the experiment uncertainties, several experiments were conducted. The experiments were conducted in the following chronological order: S3-A, S3-B, S3-C, S2, and S1. The sample was placed in its pan at the beginning of experiment S3-A. All experiments were conducted with complete heat/cool cycles as detailed in Table I. The sample was removed at the end of the five runs. In Figure 4, the differential voltage signal, dV, is shown as a function of reference temperature, T_R, for the five consecutive experiments. For the three S3 cases, only the heating is shown, including the domain with 5°C/min where melting occurs. For S2 and S1 cases, data is shown only for the first heating segment that lasts until the set point temperature reaches 600°C. The first measurement, S3-A, is very different than the subsequent four, which are almost identical. The data shown in Figure 4, indicate that, in order to insure reproducibility, the sample must undergo a melting and solidification cycle. The subsequent experiments show excellent reproducibility.

The results for T_R and dV are shown in Table V at 13 min and 28 min since the onset of each experiment. The set point rate for the times shown in Table V is 20 °C/min. In order to document the measurement uncertainty, the standard deviation was determined from the five sets of data (Table VI).

Table V. Data sampling at 13 and 28 min since the onset of measurement.

Case Id	Time [min]	T_R [°C]	dV[μV]
S3-A	13	229.20	15.88
S3-B	13	229.35	9.63
S3-C	13	228.93	9.27
S2	13	229.04	9.07
S1	13	229.53	9.15
S3-A	28	553.61	18.87
S3-B	28	553.52	11.75
S3-C	28	553.51	11.32
S2	28	553.02	11.30
S1	28	553.76	11.09

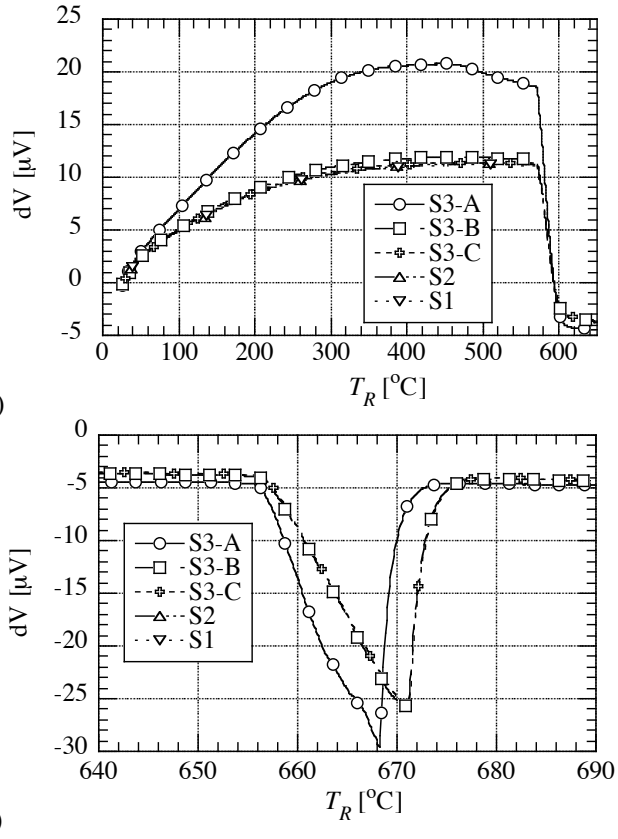

Figure 4. Differential voltage DSC signal as a function of reference temperature for temperature ranges of (a) [0:650], and (b) [640:690] [°C].

Table VI. Mean and Standard Deviation.

Time [min]	Mean (Std. Deviation) T_R [°C]	Mean (Std. Deviation) dV[μV]
13	229.21 (0.24)	9.28 (0.25)
28	553.48 (0.28)	11.36 (0.27)

CONCLUSIONS

A mathematical model was developed for the Netzsch DSC 404C instrument with high accuracy heat capacity sensor. It was assumed that each component is isothermal and that the heat transfer among components occurs by conduction

and radiation. The instrument systematic errors, which are seen in the differential signal, are considered. There is a good agreement with experimental results for baseline runs as well as for sample runs.

It was found that the lag between the furnace temperature and set point temperature is important but cannot be described by simple time-constant type equations. The proposed mathematical model yields accurate results over a wide temperature range, during heating and cooling regimes. The instrument uncertainties are described in detail. In order to insure reproducibility, the sample must undergo a melting and solidification cycle. The subsequent measurements show excellent reproducibility.

ACKNOWLEDGMENTS

This work was sponsored by the U.S. Department of Energy, Assistant Secretary for Energy Efficiency and Renewable Energy, Industrial Technologies Program, Industrial Materials for the Future (IMF), under contract DE-AC05-00OR22725 with UT-Battelle, LLC and Office of FreedomCAR and Vehicle Technologies, as part of the High Temperature Materials Laboratory User Program, Oak Ridge National Laboratory.

REFERENCES

Gray, A. P. in *Analytical Calorimetry*, ed. R. S. Porter and J. F. Johnson, Plenum Press, New York, 1968, pp. 209.

Dong, H. B. and Hunt, J. D., A Numerical Model of a Two-Pan Heat Flux DSC, Journal of Thermal Analysis and Calorimetry, Vol. 64 (2001) pp. 167-176.

Kempen, A.T.W., Sommer, F., and Mittemeijer, E. J., Calibration and Desmearing of a Differential Thermal Analysis Measurement Signal Upon Heating and Cooling, Thermochimica Acta 383 (2002) pp. 21-30.

Sabau, A.S., Porter, W.D. and Frankel, JI, "Conduction and Radiation Parameters for Analytical Models of Differential Scanning Calorimetry Instruments," *Solidification of Aluminum Alloys*, pp. 19-28, Eds. Chu, Granger, and Han, TMS, Warrendale, PA, 2004 TMS Annual Meeting, March 14-18, Charlotte, NC.

Danley, Robert L., New Heat Flux DSC Measurement Technique, Thermochimica Acta 395 (2003) pp. 201-208.

Boettinger, W. J. and U. R. Kattner, On Differential Thermal Analyzer Curves for the Melting and Freezing of Alloys, Metallurgical and Materials Transaction A, Vol. 33A, June 2002, pp. 1779-1794.

Gregory E. Osborne, Jay I. Frankel, Adrian S. Sabau, and Wallace D. Porter, "Characterization of Thermal Lags and Resistances in a Heat-Flux DSC, *Materials Processing Fundamentals*, 2004 TMS Annual Meeting, March 14-18, Charlotte, NC.